



## Research article

# Thermal lens technique's surrogacy unveiled: A novel tool for microplastic detection and quantification in water

Puthuparambil Anju Abraham<sup>a</sup>, Vijayakumar Gokul<sup>a</sup>, Mohanachandran Nair Sindhu Swapna<sup>b</sup>, Sankaranarayana Iyer Sankararaman<sup>a,\*</sup>

<sup>a</sup> Department of Optoelectronics, University of Kerala, Trivandrum, 695581, India

<sup>b</sup> Laboratory for Environmental and Life Sciences, University of Nova Gorica, Vipavska 13, Nova Gorica, SI-5000, Slovenia

## ARTICLE INFO

## Keywords:

Microplastics  
Thermal diffusivity  
Thermal lens  
Non-destructive evaluation  
Paper cup

## ABSTRACT

The escalating usage of paper cups and packaging materials with plastic coatings has evolved into a substantial environmental and health concern, evidenced by the report of microplastics in human blood. This research introduces an innovative laser-assisted thermal lens (TL) technique for the precise detection and measurement of microplastics, specifically those leaching from the inner plastic coatings of paper cups. Employing a multipronged approach encompassing scanning electron microscopy, optical microscopy, atomic force microscopy, Fourier transform infrared spectroscopy, UV-visible, and Raman spectroscopy, a comprehensive investigation is conducted into the leaching of microplastics into hot water from paper cups. The thermal diffusivity (D) of water samples containing microplastics is determined using the TL technique based on 120 observations for each temperature conducted using paper cups from three distinct manufacturers. The observation of a strong correlation between the number of microplastic particles (N) and D of the water sample enabled the setting of a linear empirical relation that can be used for computing the microplastics in water at a particular temperature. The study thus proposes a surrogate method for quantifying microplastics in water using the sensitive and non-destructive TL technique.

## 1. Introduction

Though the discovery of plastic in the twentieth century revolutionized our day-to-day life because of its low weight, good mechanical strength, and thermal and electrical insulations, its excessive use started posing a threat to the ecosystem due to its nondegradable nature. Today, the production of plastic waste has crossed 400 million tonnes, of which about 19–23 million tonnes enter into the aquatic ecosystem a year, according to the United Nations Environmental Programme. The study also estimates about 75–199 million tonnes of plastic accumulation in oceans [1]. It has many adverse effects on marine life and land-based organisms. The degradation process of plastic debris involves the formation of smaller particles known as microplastics (<5 mm in size) and even smaller nanoplastics (<100 nm in size) [2,3].

The prevalence of microplastics in the food and beverage supply chain is a growing concern with significant implications. Extensive research has documented the presence of microplastics in various food sources, including freshwater, salt, milk, fish, tea, and paper-based food packaging [4–9]. The small size of these particles facilitates their easy penetration of biological barriers, raising concerns

\* Corresponding author.

E-mail address: [drssraman@gmail.com](mailto:drssraman@gmail.com) (S.I. Sankararaman).

about ingestion, inhalation, and dermal exposure [10]. Studies indicate that individuals may unwittingly consume an average of 0.1–5 g of microplastic particles through various routes [11]. Alarmingly, recent investigations have revealed that microplastics smaller than 10  $\mu\text{m}$  can breach cell membranes and enter the circulatory system, with detections in the human placenta, breast milk, lung tissue, and sputum further underscoring the extent of plastic exposure [12–15]. Particularly worrisome is the contribution of single-use plastic materials, such as polyethylene (PE) lined paper cups, to environmental microplastic pollution. Though these cups favor convenience and hygiene benefits, they consist of a paperboard substrate (150–350  $\text{g}/\text{m}^2$ ) and a plastic liner (approximately 50  $\mu\text{m}$  thick) that can release high levels of tiny particles and harmful chemicals, including phthalates, antioxidants, perfluoroalkyl substances, and heavy metals, into the food, posing severe health risks [16–20]. Hence, urgent measures are needed to mitigate this escalating threat to food safety and human health.

Given the extensive range of challenges stemming from microplastic contamination, it is crucial to develop accurate quantification and assessment techniques. Various commonly used methods include microscopy, Fourier-transform infrared spectroscopy (FTIR), and Raman spectroscopy [21]. When Raman spectroscopy exhibits difficulty in detecting highly fluorescent, opaque, and indistinguishable polymers, FTIR's sensitivity decreases with particle size, making it less effective for detecting nano plastics [22,23]. This necessitates the development of laser-assisted sensitive, non-destructive evaluation techniques.

The thermal lens (TL) technique, renowned for its exceptional sensitivity at the nanoscale, has emerged as a powerful solution that can address the limitations of existing methods. Here, the localized heating, as a result of the pump beam absorption, results in a refractive index change in the medium, generating a lens-like effect that affects the path of the probe beam [24–26]. The TL technique enables the precise measurement of optical absorbance, surpassing the capabilities of conventional transmission spectrometry. The extraordinary signal-to-noise ratio and sensitivity allow the detection of a temperature variation of  $10^{-6}$  to  $10^{-4}$   $^{\circ}\text{C}$ , making it a valuable tool in various scientific disciplines [27]. Today, TL spectrometry, a non-destructive evaluation technique, finds applications in diversified fields like trace detection, foodstuff analysis, chemistry, environmental science, and biomedicine [27–30]. The present work comprehensively analyses the microplastics leaching into the hot water from paper cups through the multipronged approach using optical microscopy, atomic force microscopy (AFM), scanning electron microscopy (SEM), FTIR, UV-visible, and Raman spectroscopy. The paper also proposes a surrogate thermal lens-based technique for detecting and quantifying microplastics in water.

## 2. Materials and methods

To investigate the presence of microplastics leaching into the water from the paper cup, hot distilled water at different temperatures, 25  $^{\circ}\text{C}$ , 40  $^{\circ}\text{C}$ , 60  $^{\circ}\text{C}$ , 80  $^{\circ}\text{C}$ , and 95  $^{\circ}\text{C}$  is poured into the paper cups of three different manufacturing companies. The water in the cups is allowed to cool down to room temperature for 1 h. These water samples are labeled as S25, S40, S60, S80, and S95. The experiment is repeated with five sets of paper cups from three different manufacturing companies. The samples are subjected to morphological, structural, optical, and thermal characterizations.

The morphological characterization of the samples is carried out using (i) an optical microscope (Olympus CX31) at 40 $\times$  magnification, (ii) a scanning electron microscope (Carl Zeiss EVO 18 Research), and (iii) atomic force microscopy (AFM-BRUKER Dimension Edge SPM) in contact mode. The energy dispersive spectroscopic (EDS) technique using Amtech Energy Dispersive X-ray analyzer explains the sample's elemental composition. When hot water is taken in the paper cup with plastic coatings, the plastic melts

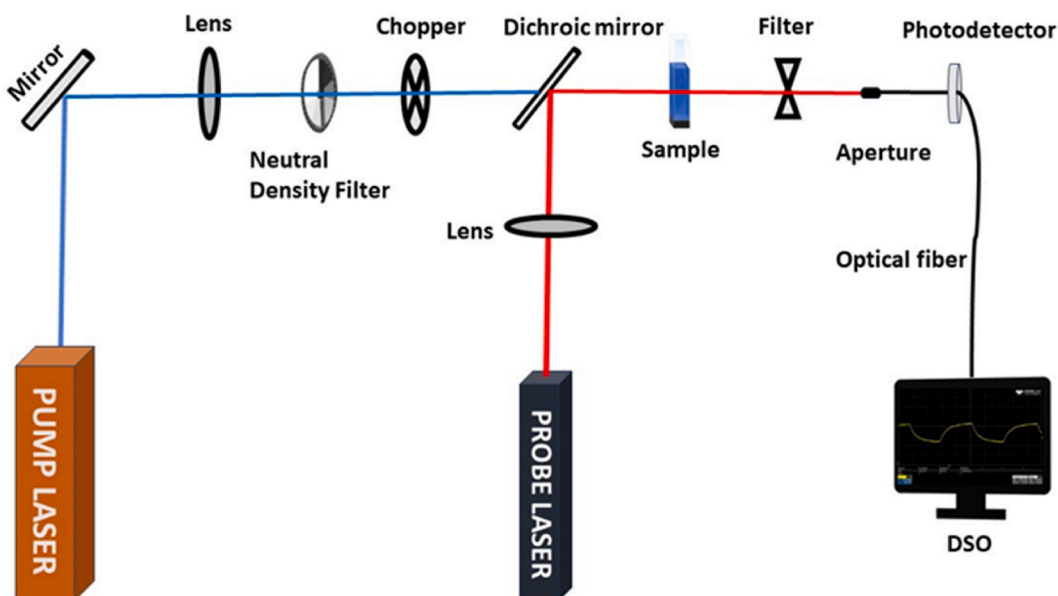


Fig. 1. Schematic representation of mode mismatched dual beam thermal lens setup.

and leaches into the water, which changes the roughness of the inner surface of the paper cup. To analyze the change in surface roughness, the hydrophobic plastic film from the inner surface is carefully peeled off to record the AFM images. To understand the structure of leached particles, the FTIR spectrum of the plastic film with S25 – S95 samples and the plastic particles collected by concentrating the sample S95 is recorded in the attenuated total reflectance mode range of  $4000\text{ cm}^{-1}$  to  $400\text{ cm}^{-1}$  using a PerkinElmer FTIR spectrophotometer. The Raman spectrum of the sample is recorded using a Horiba Lab RAM Micro-Raman Spectrometer with an argon ion laser source at 532 nm, which also helps to confirm the molecular structure. The UV–visible absorption spectrum, recorded in the range 200 nm – 800 nm using a Jasco V550 UV–visible spectrophotometer, helps in understanding the optical characteristics of the samples.

To understand and quantify the leaching of microplastics from the paper cups Neubauer counting chamber of dimension  $3\text{ mm} \times 3\text{ mm} \times 0.1\text{ mm}$ , comprising nine grids of  $1\text{ mm}^2$  is employed. The particles in the grids of the Neubauer chamber are counted by keeping the chamber under an optical microscope (Olympus CX31). From the average number of particles per grid of volume  $10^{-7}\text{ L}$  ( $1\text{ mm}^2 \times 0.1\text{ mm}$ ), the total number of particles per liter in the water sample is estimated [31].

The thermal parameter - thermal diffusivity - of the samples is determined using the mode mismatched dual beam thermal lens (MMDBTL) setup shown in Fig. 1. An average of 120 TL signals collected from five sets of paper cups from each company have been analyzed for the TL study at each temperature. In the arrangement, a TEM<sub>00</sub> mode Kimmon IK series Helium–Cadmium laser (wavelength  $\lambda_e = 442\text{ nm}$ , power = 80 mW) and a Helium–Neon laser (wavelength  $\lambda_p = 632.8\text{ nm}$ , power = 2 mW) are used to set up a collinear MMDBTL configuration. The 442 nm laser is the pump beam, while the 632.8 nm laser is the probe beam for the MMDBTL setup. The pump beam intensity is reduced to get a blooming-free TL formation inside the sample using a neutral density filter. Intensity modulation of the pump beam at 1 Hz is achieved using an electromechanical chopper (SRS – 540). The focused pump beam is directed onto a 10 mm glass cuvette (sample cell length, l) containing the sample by a convex lens of focal length 40 cm. Simultaneously, the low-intensity probe beam is directed onto the sample centre collinearly with the pump beam through a dichroic mirror. The TL formation due to the probe beam is neglected, as the nanofluid shows poor absorption at the  $\lambda_p$ . The degree of mode mismatching ( $m = \left(\frac{\omega_p}{\omega_e}\right)^2$ ) is determined by the ratio of the squares of the probe beam ( $\omega_p = 1.4\text{ mm}$ ) and pump beam ( $\omega_e = 0.236\text{ mm}$ ) radii at the sample centre calculated by using the Nano Scan 2S commercial slit beam profiler. The variations in the central beam intensity of the probe beam are analyzed using a photodetector. The resulting TL signals from the photodetector are displayed on a digital storage oscilloscope, Teledyne Wave Surfer (DSO, 500 MHz).

Let  $I_0$  be the intensity of the probe beam centre at a time  $(t) = 0$ , and  $I(t)$  be the intensity for a particular instant  $t$ . The central intensity variation can be expressed as an equation (1) [32].

$$I(t) = I_0 \left\{ \left[ 1 - \frac{\theta}{2} \tan^{-1} \left( \frac{2mV}{\left[ (1 + 2m)^2 + V^2 \right] \left( \frac{t}{t_c} \right) + 1 + 2m + V^2} \right) \right]^2 \right\} \quad (1)$$

here,  $t_c$  stands for the characteristic time constant, and  $V$  represents the ratio of the separation between the sample cell and the probe beam waist to the confocal distance of the probe beam. The parameter  $\theta$  depends on the quantities  $P_{th}$ - absorbed photothermal energy,  $A$  - absorption coefficient of the sample,  $\frac{dn}{dT}$  - refractive index gradient with respect to the temperature, and  $K$ -thermal conductivity by equation (2) [32,33].

$$\theta = - \frac{P_{th} A l \frac{dn}{dT}}{K \lambda_p} \quad (2)$$

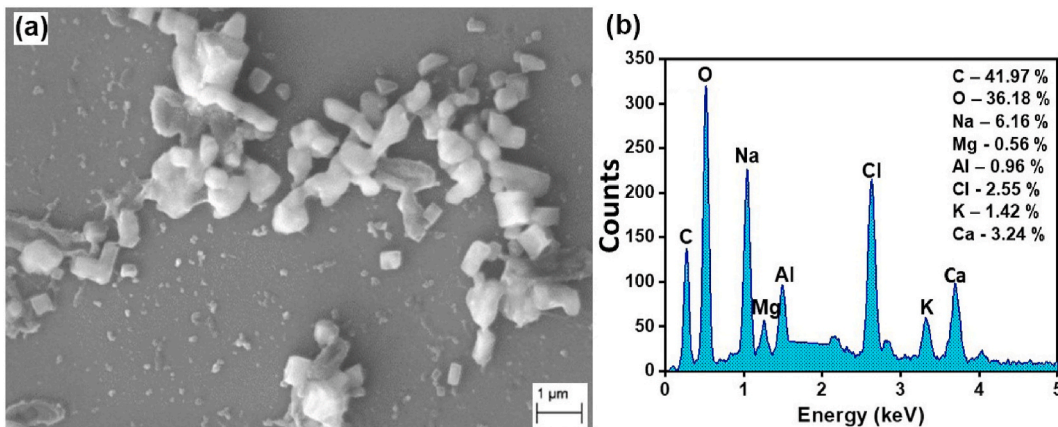


Fig. 2. (a) SEM image of the sample S95 (b) EDS spectrum of the sample S95 with atomic % of elements present.

The experimental TL signal is subjected to curve fitting using equation (1). The sample's thermal diffusivity (D) can be calculated using equation (3) [32,33],

$$D = \frac{(\omega_e)^2}{4t_c} \quad (3)$$

### 3. Results and discussion

The fact that paper cups have a fine coating of HDPE suggests the possibility of leaching microplastics into the hot liquid taken in them. To verify the presence of any such particle in the liquid, here water, SEM, and optical microscopic analysis are carried out. The study helps in understanding the morphology and number density of particles present. The SEM image shown in Fig. 2a reveals the presence of spherical particles at the micron size along with an increased concentration of nanosized particles when hot water at a temperature of 95 °C is poured into the paper cup. The quantification of microparticles in samples S40 to S95 is conducted using an optical microscope, and the revealing number density of particles is 21.4 million/liter, 41.6 million/liter, 75.2 million/liter, and 109.4 million/liter, respectively. The observation reveals a positive correlation between the number of microparticles in the sample and the initial temperature of water taken in the paper cup.

Having found micron and nano-sized particles in the samples, investigations are carried out to understand the nature and structure of the particles by various techniques like UV-visible, FTIR, Raman, and EDS. Elemental analysis of the S95 by EDS confirms the presence of carbon, oxygen, chlorine, magnesium, aluminum, sodium, potassium, and calcium, as shown in Fig. 2b. The presence of carbon, constituting 41.97 % of the atomic weight, suggests that the particles in water leached from the paper cup could be microplastics which should be confirmed through further spectroscopic analyses. Ranjan et al. [34], have reported that elements other than carbon and oxygen in the samples can be attributed to the leaching of several additives used in the paper cups to enhance the plastic coatings' flexibility, colour, and durability. The literature on microplastics [34] supports the elements listed in Fig. 2b as the possible constituents of the coating material in the paper cup.

The UV-visible absorption spectrum reveals electronic transitions from the ground to the excited state. The absorption spectrum of samples S25, S40, S60, S80, and S95, shown in Fig. 3, exhibits a peak at 263 nm. This spectrum aligns with reported results, and the 263 nm peak is attributed to the  $\pi - \pi^*$  transition, signifying electron delocalization in an aromatic ring [35]. The UV-visible absorption spectrum (Fig. 3) agrees well with the literature reports of microplastics thereby suggesting the particles found in the samples to be microplastics. The increase of the absorbance at 263 nm for the samples S25 – S95 indicates the increase of microplastic leaching into the water.

Fourier-transform infrared spectroscopy is a non-destructive method that provides information about a sample's chemical composition, molecular structure, and functional groups. The representative FTIR spectrum of the high-density polyethylene(HDPE) films peeled off from the paper cups with S25 – S95 is shown in Fig. 4a. Fig. 4b shows the FTIR spectrum of the HDPE particles collected from the samples S95. The peaks at 2916  $\text{cm}^{-1}$  and 2848  $\text{cm}^{-1}$  can be allocated to the CH stretching of all hydrocarbon constituents in polymers [36–38]. The peaks located at 1472  $\text{cm}^{-1}$  and 1462  $\text{cm}^{-1}$  correspond to  $\text{CH}_2$  bending and C–H deformation, while those at 729  $\text{cm}^{-1}$  and 718  $\text{cm}^{-1}$  belong to  $\text{CH}_2$  rocking vibrations [35,37]. Except for the peak at 2916  $\text{cm}^{-1}$ , all other peaks found in the hydrophobic film and S95, match the absorption peaks of HDPE reported in the literature. The cellulosic peak at 3381  $\text{cm}^{-1}$  in the hydrophobic film and those in the range 1200  $\text{cm}^{-1}$ –800  $\text{cm}^{-1}$  observed in the film and S95 indicate the possibility of the fraction of paper adhered to the plastic film [39,40]. Thus, the FTIR spectrum showing the characteristic peaks of HDPE confirms the presence of microplastics leaching from the paper cup. Table 1 presents the peak assignments of polymers identified in the hydrophobic film and the sample S95.

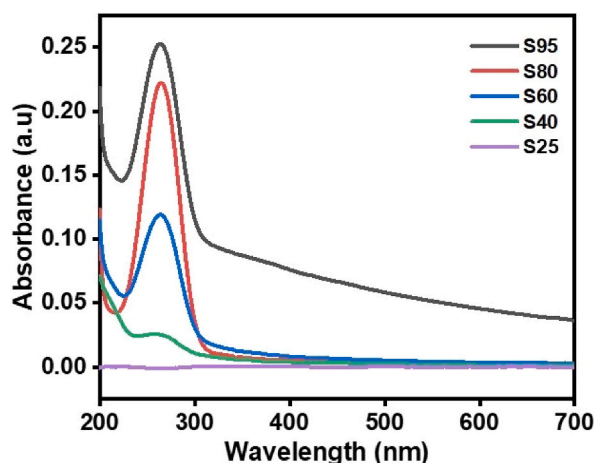


Fig. 3. UV-visible spectrum of the sample S25 – S95.

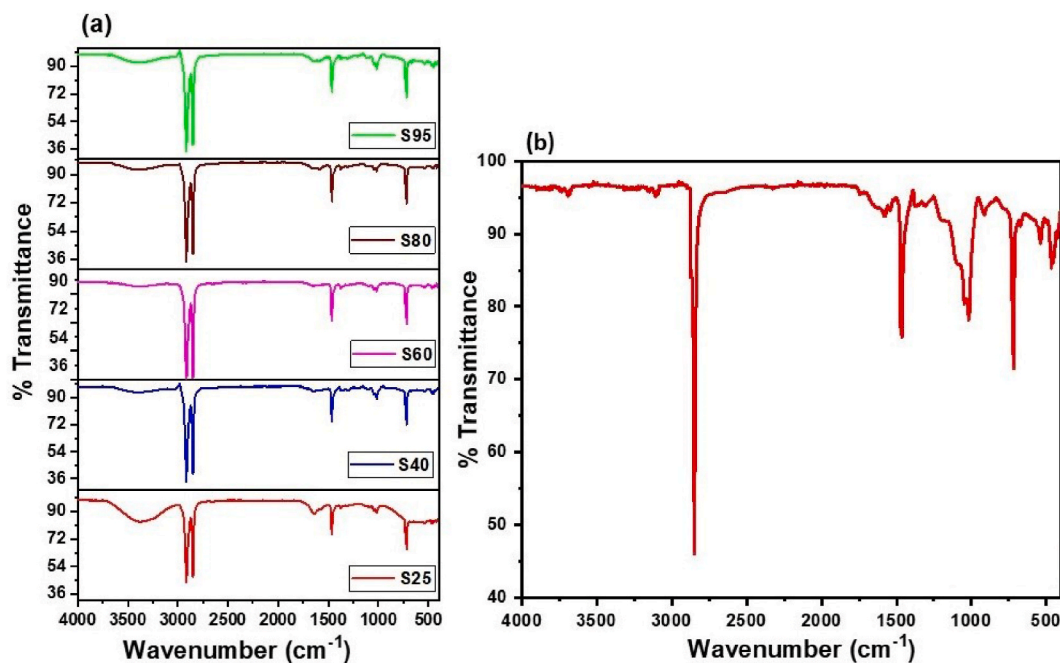


Fig. 4. FTIR spectrum of the samples – (a) HDPE films peeled off from the paper cups with S25–S95 and (b) HDPE particles collected from the sample S95.

Raman spectroscopy deciphers the sample's molecular vibrations, rotations, and other low-frequency modes. The Raman spectrum of the sample S95 (Fig. 5) exhibits characteristic peaks at  $2891\text{ cm}^{-1}$  and  $2895\text{ cm}^{-1}$ , attributed to  $\text{CH}_2$  stretching and CH symmetrical stretching, respectively, signifying the presence of aliphatic hydrocarbon components [41]. Notably, the appearance of the peak at  $1094\text{ cm}^{-1}$  corresponds to the anti-symmetric stretching vibration of C–O–C bonds, suggesting the ether linkages within the microplastic composition [41]. The  $1052\text{ cm}^{-1}$  peak denotes CH bending and C–C stretching modes, shedding light on the structural characteristics of the microplastics. The spectrum further reveals peaks at  $1118\text{ cm}^{-1}$ ,  $1604\text{ cm}^{-1}$ ,  $1418\text{ cm}^{-1}$ ,  $1449\text{ cm}^{-1}$ ,  $1599\text{ cm}^{-1}$ ,  $990\text{ cm}^{-1}$ , and  $906\text{ cm}^{-1}$ , corresponding to CH in-plane bending, C=C stretching,  $\text{CH}_2$  wagging,  $\text{CH}_2$  scissoring, C=C stretching, C–C, C–OH, C–H vibrations, and C–H out-of-plane deformation, respectively [40,42,43]. These spectral signatures confirm the leaching of microplastics from the paper cup into the water.

When water at different temperatures is taken in the paper cup, the microplastic particles leach into the water. This process alters the surface morphology of the HDPE film coated inside the paper cup. The leaching-induced surface modifications are displayed in the AFM images shown in Fig. 6. The AFM analysis reveals that root means square roughness varies from 138 nm to 270 nm for the fresh film and that with S95, respectively reiterating the dilapidation of the film due to the leaching of microplastics into the water.

In the present work, for the first time, the TL technique is used as a valuable tool for investigating microplastic leaching from a paper cup into water. The thermal diffusivity of the samples is studied to characterize the variation in the water due to the leaching of

Table 1  
FTIR spectral peak assignments of fresh film and S95.

Wavenumber ( $\text{cm}^{-1}$ )	Fresh Film	S95	Assignment	References
3381	✓	x	O–H stretching of carboxylic acids	[39,40]
2916	✓	x	CH stretching	[36]
2848	✓	✓	CH stretching	[38]
1747	x	✓	C–O stretching	[38]
1643	✓	x	C–C stretching	[36]
1580	x	✓	C–C stretching	[38]
1540	x	✓	C–N stretching	
1462	✓	✓	C–H deformation, C–H bending	[38]
1472	✓	✓	C–H deformation	[38]
1376	✓	✓	$\text{CH}_3$ bending	[36]
1048	✓	✓	C–O stretching	[36,39]
1017	✓	✓	C–O stretching	[36]
729	✓	✓	C–H rocking	[36]
718	✓	✓	C–H rocking	[36]
540	✓	✓	aromatic ring out of the plane bending	[38]



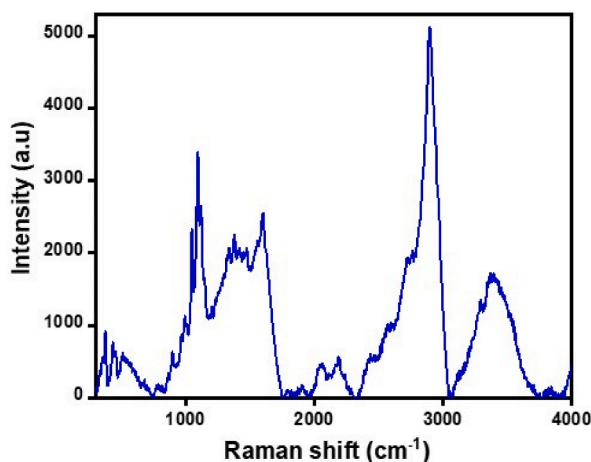


Fig. 5. Raman spectrum of S95.

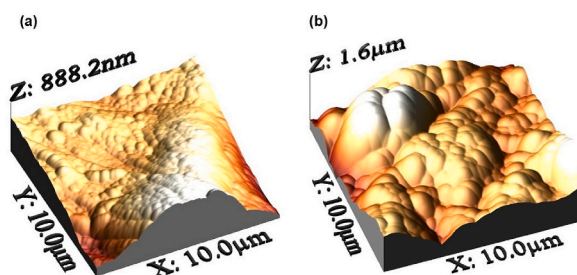


Fig. 6. AFM 3-D image of the surface of the hydrophobic film (a) before taking hot water, (b) after taking hot water.

microplastics. The thermal diffusivity of a paper cup holding hot water at different temperatures is analyzed by the highly sensitive MMDBT technique. Initially, the TL setup is standardized by finding the  $D$  value of the water (S25), and its value is obtained as  $(1.43 \pm 0.01) \times 10^{-7} \text{ m}^2/\text{s}$ , which agrees well with literature reports [44].

For the thermal diffusivity study, a total of 480 signals are analyzed. The boxplot representation of 120 TL signals at each temperature for five sets of paper cups (3 different manufacturing companies each) is shown in Fig. 7. After obtaining an average of 120 thermal lens signals, the values of  $D$  for the samples S25 – S95 are shown in Fig. 8a. It can be seen that the thermal diffusivity gradually increases from S25 to S95. This rise in  $D$  primarily stems from the higher number density of leached microplastic particles at higher temperatures due to intensified Brownian motion, better dispersion, increased interfacial interactions, and variations in particle size [45–47]. Sankar-Swapna model explains the generalized theory of thermal conductivity for different media. The model explains the effective thermal conduction of solids, different solid combinations, and, solid-fluid mixtures. As the volume of solid particles in the liquid increases, the particle concentration along the direction of propagation of heat increases, leading to the enhancement of effective conduction through the medium [48]. The thermal diffusivity enhancement of the samples observed in the study is due to the increase in the number of micro/nano plastics and the consequent increase of solid volume fraction which is in good agreement with the Sankar-Swapna model. The optical microscopic analysis, revealing the increase of the number of particles and the ensuing increased optical absorbance reflected in the UV-visible absorption spectrum, also justifies the observed increase of  $D$ . The variation of  $D$  of the water sample containing microplastics is found to follow the linear relation, given by equation (4), with the temperature  $T$  of the water while pouring into the paper cup.

$$D = 3 \times 10^{-10}T + 1 \times 10^{-7} \text{ (m}^2/\text{s)} \quad (4)$$

The optical microscope analysis shows a quantification of the number of microplastics ( $N$ ) in 1 L of water samples at different temperatures  $T$  (S25 – S95). The degree of correlation of  $N$  with  $D$  can be understood by plotting the thermal diffusivity of the samples against the number of microplastics in 1 L of water samples, as shown in Fig. 8b. From Fig. 8b, it is evident that  $D$  is strongly correlated to  $N$  through the linear relation given by equation (5) with  $R^2 = 0.99$ .

$$N \text{ (million / litre)} = 5 \times 10^9 D - 7 \times 10^2 \quad (5)$$

Equation (5) can be used for finding the number of microplastics ( $N$ ) knowing the thermal diffusivity of the sample by TL technique. Thus, the present work proposes a novel surrogate method for estimating the number of microplastics in water samples using the sensitive, non-destructive TL technique.

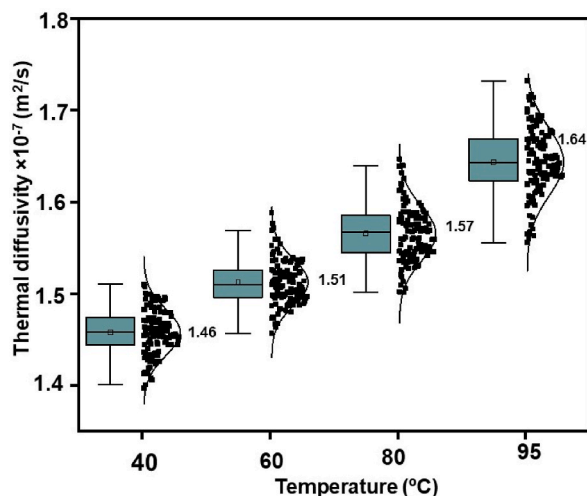


Fig. 7. Boxplot representation of thermal diffusivity of the sample S40-S95.

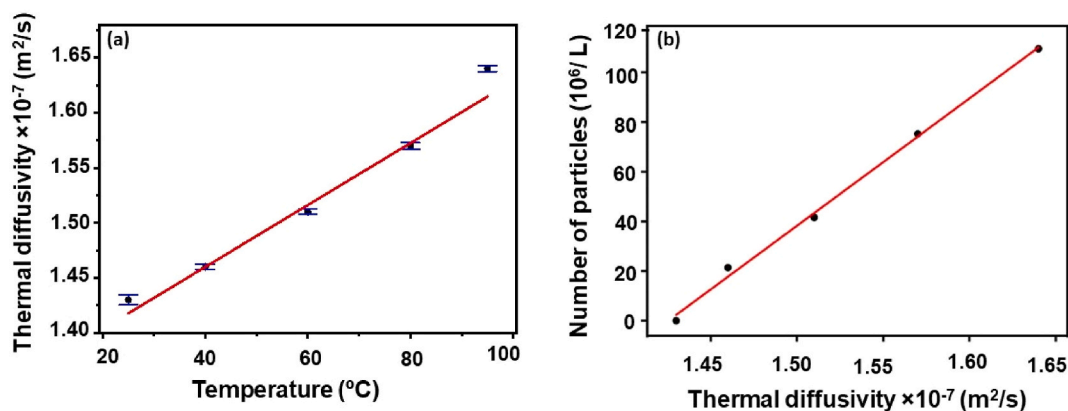


Fig. 8. (a) Thermal diffusivity at different temperatures, (b) correlation of number of particles and thermal diffusivity.

#### 4. Conclusions

Plastic, a substance that has greatly enriched our daily lives and played a pivotal role in the evolution of urban living, has emerged as both a beloved companion and a contentious adversary, as it encompasses a diverse array of modern polymers, requiring a continuous assessment to safeguard our environment from its potential perils. The paper unveils the potential of the TL technique in detecting and quantifying microplastics. The microplastic leaching into water from the inner HDPE coatings is systematically investigated by various techniques. The morphology of the microplastics is understood from optical microscope and SEM images. The SEM images showcase the presence of spherical microparticles with the highest concentration at 95 °C. EDS analysis suggests the presence of microplastic, with carbon constituting 41.97 % of the atomic weight. The UV-visible absorption spectrum exhibited a prominent 263 nm peak, linked to the  $\pi$ - $\pi^*$  transition signifying electron delocalization in an aromatic ring, and its intensity increased with rising temperatures, indicating a temperature-microplastic release correlation. The FTIR analysis identified HDPE-based microplastics and cellulose-related peaks, supporting the likelihood of microplastic leaching from the cup. Raman spectroscopy unveiled microplastic composition and structural insights, detecting distinctive peaks associated with aliphatic hydrocarbons, ether linkages, and structural features. The analysis of microplastic particles reveals a direct relationship between water temperature and leaching, with 109.4 million particles per liter detected in S95. The AFM analysis of plastic film exposed to hot water demonstrates significant surface roughness changes, signifying structural deterioration due to heat exposure. The thermal diffusivity of the water samples with microplastics is determined from the 120 observations, performed with the paper cups of three different manufacturers, by the TL technique. It is observed that the thermal diffusivity exhibits a linear correlation with the temperature of the water taken in the paper cup. The number of microplastics leached into water samples also exhibited a linear correlation with thermal diffusivity. Thus, the study proposes a surrogate sensitive, non-destructive TL -based technique for detecting and quantifying microplastics.

## CRedit authorship contribution statement

**Puthuparambil Anju Abraham:** Writing – original draft, Methodology, Formal analysis, Data curation. **Vijayakumar Gokul:** Writing – review & editing, Software, Investigation, Formal analysis. **Mohanachandran Nair Sindhu Swapna:** Writing – review & editing, Validation, Supervision, Formal analysis. **Sankaranarayana Iyer Sankaraman:** Writing – review & editing, Visualization, Supervision, Formal analysis, Conceptualization.

## Declaration of competing interest

The authors declare that they have no known competing financial interests or personal relationships that could have appeared to influence the work reported in this paper.

## Acknowledgments

Acknowledging Central Laboratory for Instrumentation and Facilitation (CLIF), University of Kerala, Trivandrum, 695581, India, for providing an instrumentation facility.

## References

- [1] UNEP, From Pollution to Solution: a global assessment of marine litter and plastic pollution. <https://www.unep.org/resources/pollution-solution-global-assessment-marine-litter-and-plastic-pollution>, 2021. (Accessed 10 September 2023).
- [2] J.P. Da Costa, A. Paço, P.S.M. Santos, A.C. Duarte, T. Rocha-Santos, Microplastics in soils: assessment, analytics and risks, *Environ. Chem.* 16 (2019) 18–30, <https://doi.org/10.1071/EN18150>.
- [3] NOAA, What are microplastics. <https://oceanservice.noaa.gov/facts/microplastics.html>, 2023. (Accessed 8 September 2023).
- [4] A.A. Koelmans, N.H. Mohamed Nor, E. Hermsen, M. Kooi, S.M. Mintenig, J. De France, Microplastics in freshwaters and drinking water: critical review and assessment of data quality, *Water Res.* 155 (2019) 410–422, <https://doi.org/10.1016/j.watres.2019.02.054>.
- [5] L.M. Hernandez, E.G. Xu, H.C.E. Larsson, R. Tahara, V.B. Maisuria, N. Tufenkji, Plastic teabags release billions of microparticles and nanoparticles into tea, *Environ. Sci. Technol.* 53 (2019) 12300–12310, <https://doi.org/10.1021/acs.est.9b02540>.
- [6] C. Pironti, M. Ricciardi, O. Motta, Y. Miele, A. Proto, L. Montano, Microplastics in the environment: intake through the food web, human exposure and toxicological effects, *Toxics* 9 (2021) 1–29, <https://doi.org/10.3390/toxics9090224>.
- [7] E. Danopoulos, L. Jenner, M. Twiddy, J.M. Rotchell, Microplastic contamination of salt intended for human consumption: a systematic review and meta-analysis, *SN Appl. Sci.* 2 (2020) 1–18, <https://doi.org/10.1007/s42452-020-03749-0>.
- [8] F. Collard, B. Gilbert, G. Eppe, E. Parmentier, K. Das, Detection of anthropogenic particles in fish stomachs: an isolation method adapted to identification by Raman spectroscopy, *Arch. Environ. Contam. Toxicol.* 69 (2015) 331–339, <https://doi.org/10.1007/s00244-015-0221-0>.
- [9] C.D. Zangmeister, J.G. Radney, K.D. Benkstein, B. Kalanyan, Common single-use consumer plastic products release trillions of sub-100 nm nanoparticles per liter into water during normal use, *Environ. Sci. Technol.* 56 (2022) 5448–5455, <https://doi.org/10.1021/acs.est.1c06768>.
- [10] L. Rubio, R. Marcos, A. Hernández, Potential adverse health effects of ingested micro- and nanoplastics on humans. Lessons learned from in vivo and in vitro mammalian models, *J. Toxicol. Environ. Health Part B Crit. Rev.* 23 (2020) 51–68, <https://doi.org/10.1080/10937404.2019.1700598>.
- [11] K. Senathirajah, S. Attwood, G. Bhagwat, M. Carbery, S. Wilson, T. Palanisami, Estimation of the mass of microplastics ingested – a pivotal first step towards human health risk assessment, *J. Hazard Mater.* 404 (2021) 124004, <https://doi.org/10.1016/j.jhazmat.2020.124004>.
- [12] A. Ragusa, A. Svelato, C. Santacroce, P. Catalano, V. Notarstefano, O. Carnevali, F. Papa, M.C.A. Rongioletti, F. Baiocco, S. Draghi, E. D'Amore, D. Rinaldo, M. Matta, E. Giorgini, Placentia: first evidence of microplastics in human placenta, *Environ. Int.* 146 (2021) 106274, <https://doi.org/10.1016/j.envint.2020.106274>.
- [13] A. Ragusa, V. Notarstefano, A. Svelato, A. Belloni, G. Gioacchini, C. Blondeel, E. Zucchelli, C. De Luca, S. D'Avino, A. Gulotta, O. Carnevali, E. Giorgini, Raman microspectroscopy detection and characterisation of microplastics in human breastmilk, *Polymers* 14 (2022) 1–14, <https://doi.org/10.3390/polym14132700>.
- [14] A. Ragusa, M. Matta, L. Cristiano, R. Matassa, E. Battaglione, A. Svelato, C. De Luca, S. D'Avino, A. Gulotta, M.C.A. Rongioletti, P. Catalano, C. Santacroce, V. Notarstefano, O. Carnevali, E. Giorgini, E. Vizza, G. Familiari, S.A. Nottola, Deeply in plasticenta: presence of microplastics in the intracellular compartment of human placentas, *Int. J. Environ. Res. Publ. Health* 19 (2022), <https://doi.org/10.3390/ijerph191811593>.
- [15] S. Huang, X. Huang, R. Bi, Q. Guo, X. Yu, Q. Zeng, Z. Huang, T. Liu, H. Wu, Y. Chen, J. Xu, Y. Wu, P. Guo, Detection and analysis of microplastics in human sputum, *Environ. Sci. Technol.* 56 (2022) 2476–2486, <https://doi.org/10.1021/acs.est.1c03859>.
- [16] N. Triantafillopoulos, A.A. Koukoulas, The future of single-use paper coffee cups: current progress and outlook, *Bioresources* 15 (2020) 7260–7287, <https://doi.org/10.15376/biores.15.3.Triantafillopoulos>.
- [17] M.J. Lopez-Espinosa, A. Granada, P. Araque, J.M. Molina-Molina, M.C. Puertollano, A. Rivas, M. Fernández, I. Cerrillo, M.F. Olea-Serrano, C. López, N. Olea, Oestrogenicity of paper and cardboard extracts used as food containers, *Food Addit. Contam.* 24 (2007) 95–102, <https://doi.org/10.1080/02652030600936375>.
- [18] J.I. Chang, Y.J. Chen, Effects of bulking agents on food waste composting, *Bioresour. Technol.* 101 (2010) 5917–5924, <https://doi.org/10.1016/j.biortech.2010.02.042>.
- [19] M. Xue, X.S. Chai, X. Li, R. Chen, Migration of organic contaminants into dry powdered food in paper packaging materials and the influencing factors, *J. Food Eng.* 262 (2019) 75–82, <https://doi.org/10.1016/j.jfoodeng.2019.05.018>.
- [20] P. Bhatt, V.M. Pathak, A.R. Bagheri, M. Bilal, Microplastic contaminants in the aqueous environment, fate, toxicity consequences, and remediation strategies, *Environ. Res.* 200 (2021) 111762, <https://doi.org/10.1016/j.envres.2021.111762>.
- [21] F. Glöckler, F. Foschum, A. Kienle, Continuous sizing and identification of microplastics in water, *Sensors* 23 (2023), <https://doi.org/10.3390/s23020781>.
- [22] B.O. Asamoah, E. Uurasjärvi, J. Rätty, A. Koistinen, M. Roussey, K.E. Peiponen, Towards the development of portable and in situ optical devices for detection of micro and nanoplastics in water: a review on the current status, *Polymers* 13 (2021) 1–30, <https://doi.org/10.3390/polym13050730>.
- [23] A. Baruah, A. Sharma, S. Sharma, R. Nagrai, An insight into different microplastic detection methods, *Int. J. Environ. Sci. Technol.* 19 (2022) 5721–5730, <https://doi.org/10.1007/s13762-021-03384-1>.
- [24] M. Franko, C.D. Tran, Thermal lens spectroscopy, *encycl. Anal. Chem.* (2010) 1–32, <https://doi.org/10.1002/9780470027318.a9079>.
- [25] M. Franko, C.D. Tran, Analytical thermal lens instrumentation, *Rev. Sci. Instrum.* 67 (1996) 1–18, <https://doi.org/10.1063/1.1147512>.
- [26] J.P. Gordon, R.C.C. Leite, R.S. Moore, S.P.S. Porto, J.R. Whinnery, Long-transient effects in lasers with inserted liquid samples, *J. Appl. Phys.* 36 (1965) 3–8, <https://doi.org/10.1063/1.1713919>.
- [27] M.N. Sindhu Swapna, V. Raj, H. Cabrera, S.I. Sankaraman, Thermal lensing of multi-walled carbon nanotube solutions as heat transfer nanofluids, *ACS Appl. Nano Mater.* 4 (2021) 3416–3425, <https://doi.org/10.1021/acsanm.0c03219>.
- [28] S.C. Hall, *Loyola eCommons Rotoreflected Double-Beam Thermal Lens Spectrometry and Simultaneous Thermal Lens and Fluorescence Detection for High Performance Microbore Liquid Chromatography*, 1989.



- [29] S. Luterotti, M. Franko, D. Bicanic, Ultrasensitive determination of  $\beta$ -carotene in fish oil-based supplementary drugs by HPLC-TLS, *J. Pharm. Biomed. Anal.* 21 (1999) 901–909, [https://doi.org/10.1016/S0731-7085\(99\)00185-5](https://doi.org/10.1016/S0731-7085(99)00185-5).
- [30] M. Franko, L. Goljat, M. Liu, H. Budasheva, M. Žorž Furlan, D. Korte, Recent progress and applications of thermal lens spectrometry and photothermal beam deflection techniques in environmental sensing, *Sensors* 23 (2023), <https://doi.org/10.3390/s23010472>.
- [31] J.C. Prata, C. Venâncio, J.P. da Costa, I. Lopes, A.C. Duarte, T. Rocha-Santos, Considerations when using microplates and Neubauer counting chamber in ecotoxicity tests on microplastics, *Mar. Pollut. Bull.* 170 (2021), <https://doi.org/10.1016/j.marpolbul.2021.112615>.
- [32] J. Shen, R.D. Lowe, R.D. Snook, A model for cw laser induced mode-mismatched dual-beam thermal lens spectrometry, *Chem. Phys.* 165 (1992) 385–396, [https://doi.org/10.1016/0301-0104\(92\)87053-C](https://doi.org/10.1016/0301-0104(92)87053-C).
- [33] V. Gokul, M.N.S. Swapna, G. Ambadas, S.I. Sankararaman, Development of semiconducting graphitic carbon nitride nanofluid for heat transfer applications: a mode mismatched thermal lens study, *Diam. Relat. Mater.* 138 (2023) 110215, <https://doi.org/10.1016/j.diamond.2023.110215>.
- [34] V.P. Ranjan, A. Joseph, S. Goel, Microplastics and other harmful substances released from disposable paper cups into hot water, *J. Hazard Mater.* 404 (2021) 124118, <https://doi.org/10.1016/j.jhazmat.2020.124118>.
- [35] G.C. del Pizarro, O.G. Marambio, M. Jeria-Orell, C.M. González-Henríquez, M. Sarabia-Vallejos, K.E. Geckeler, Effect of annealing and UV-radiation time over micropore architecture of self-assembled block copolymer thin film, *Express Polym. Lett.* 9 (2015) 525–535, <https://doi.org/10.3144/expresspolymlett.2015.50>.
- [36] R. Chércoles Asensio, M. San Andrés Moya, J.M. De La Roja, M. Gómez, Analytical characterization of polymers used in conservation and restoration by ATR-FTIR spectroscopy, *Anal. Bioanal. Chem.* 395 (2009) 2081–2096, <https://doi.org/10.1007/s00216-009-3201-2>.
- [37] C.B. Lauridsen, L.W. Hansen, T. Brock-Nannestad, J. Bendix, K.P. Simonsen, A study of stearyl alcohol bloom on Dan Hill PVC dolls and the influence of temperature, *Stud. Conserv.* 62 (2017) 445–455, <https://doi.org/10.1080/00393630.2016.1206651>.
- [38] M.R. Jung, F.D. Horgen, S.V. Orski, V. Rodriguez C, K.L. Beers, G.H. Balazs, T.T. Jones, T.M. Work, K.C. Brignac, S.J. Royer, K.D. Hyrenbach, B.A. Jensen, J. M. Lynch, Validation of ATR FT-IR to identify polymers of plastic marine debris, including those ingested by marine organisms, *Mar. Pollut. Bull.* 127 (2018) 704–716, <https://doi.org/10.1016/j.marpolbul.2017.12.061>.
- [39] L.M. Ilharco, R. Brito De Barros, Aggregation of pseudoisocyanine iodide in cellulose acetate films: structural characterization by FTIR, *Langmuir* 16 (2000) 9331–9337, <https://doi.org/10.1021/la000579e>.
- [40] L. Wang, Q. Zhou, X. Ji, J. Peng, H. Nawaz, G. Xia, X. Ji, J. Zhang, J. Zhang, Fabrication and characterization of transparent and uniform cellulose/polyethylene composite films from used disposable paper cups by the “one-pot method,” *Polymers* 14 (2022) <https://doi.org/10.3390/polym14061070>.
- [41] N. Jin, Y. Song, R. Ma, J. Li, G. Li, D. Zhang, Characterization and identification of microplastics using Raman spectroscopy coupled with multivariate analysis, *Anal. Chim. Acta* 1197 (2022) 339519, <https://doi.org/10.1016/j.aca.2022.339519>.
- [42] S. Unnimaya, N. Mithun, J. Lukose, M.P. Nair, A. Gopinath, S. Chidangil, Identification of microplastics using a custom built micro-Raman spectrometer, *J. Phys. Conf. Ser.* 2426 (2023), <https://doi.org/10.1088/1742-6596/2426/1/012007>.
- [43] T.H. Lippert, F. Zimmermann, A. Wokaun, Surface analysis of excimer-laser-treated polyethylene-terephthalate by surface-enhanced Raman scattering and X-ray photoelectron spectroscopy, *Appl. Spectrosc.* 47 (1993) 1931–1942, <https://doi.org/10.1366/0003702934065911>.
- [44] M.S. Swapna, S. Sankararaman, Organometallic sodium carbide for heat transfer applications: a thermal lens study, *Int. J. Thermophys.* 41 (2020) 1–13, <https://doi.org/10.1007/s10765-020-02675-y>.
- [45] R.S. Vajjha, D.K. Das, A review and analysis on influence of temperature and concentration of nanofluids on thermophysical properties, heat transfer and pumping power, *Int. J. Heat Mass Transf.* 55 (2012) 4063–4078, <https://doi.org/10.1016/j.ijheatmasstransfer.2012.03.048>.
- [46] S. Mukherjee, P.C. Mishra, P. Chaudhuri, S. Chakraborty, Contributory effect of diffusive heat conduction and Brownian motion on thermal conductivity enhancement of nanofluids, *Pramana - J. Phys.* 94 (2020), <https://doi.org/10.1007/s12043-020-02008-6>.
- [47] V. Gokul, M.S. Swapna, V. Raj, H.V. Saritha Devi, S. Sankararaman, Concentration-dependent thermal duality of hafnium carbide nanofluid for heat transfer applications: a mode mismatched thermal lens study, *Int. J. Thermophys.* 42 (2021) 1–12, <https://doi.org/10.1007/s10765-021-02859-0>.
- [48] S. Mohanachandran Nair Sindhu, S. Sankaranarayana Iyer, Generalized theory of thermal conductivity for different media: solids to nanofluids, *J. Phys. Chem. C* 123 (2019) 23264–23271, <https://doi.org/10.1021/acs.jpcc.9b07406>.